International Journal of Thermophysics, Vol. 19, No. 1, 1998

Ideal-Gas Heat Capacities and Virial Coefficients of HFC Refrigerants

A. Yokozeki,[1,2] H. Sato,[1] and K. Watanabe[1,3]

Received August 26, 1997

Thermodynamic properties of HFC (hydrofluorocarbon) compounds have been extensively studied with worldwide interest as alternative refrigerants. Both quality and quantity in the experimental data far exceed those for the CFC and HCFC refrigerants. These data now provide a great opportunity to examine the validity of theoretical models, and vice versa. Among them, the ideal-gas heat capacity (C_p^0) and virial coefficients derived from the experimental data are of particular interest, since they are directly related to the intramolecular and intermolecular potentials through the statistical mechanical procedure. There have been some discrepancies reported in the observed and theoretical C_p^0 for HFC compounds. We have performed new calculations of C_p^0 for several HFCs. The present results are consistent with the selected experimental values. The second (B) and third (C) virial coefficients have been reported for these HFC refrigerants from speed of sound data and Burnett PVT data. Often, a square well-type intermolecular potential is employed to correlate the data. However, the model potential cannot account consistently for both B and C coefficients with the same potential parameters. We have analyzed the data with the Stockmayer potential and obtained self-consistent results for various HFC (R-23, R-32, R-125, R-134a, R-143a, and R-152a) compounds with physically reasonable potential parameters.

KEY WORDS: ideal gas; heat capacity; hydrofluorocarbons; Stockmayer potential; virial coefficient.

[1] Department of System Design Engineering, Faculty of Science and Technology, Keio University, 3-14-1 Hiyoshi, Kohoku-ku, Yokohama 223, Japan.

[2] Invited visiting professor at Keio University from DuPont Fluoroproducts Laboratory, Wilmington, Delaware, U.S.A.

[3] To whom correspondence should be addressed.

0195-928X/00/0700-0089$18.00/0

1. INTRODUCTION

As alternative refrigerants to the ozone-depleting CFCs, hydrofluorocarbons (HFC) have been proposed: R-134a (CF_3CH_2F) for R-12, binary or ternary mixtures of R-32 (CH_2F_2), R-125 (CF_3CHF_2), and R-134a for R-22, binary or ternary mixtures of R-125, R-143a (CF_3CH_3), and R-134a for R-502, and so forth. Developing new refrigerants requires enormous effort: chemical production, toxicity and safety tests, material stability and compatibility tests, lubricant selection, new compressor/equipment design and testing, cost estimation, and energy efficiency tests. In each step of development, fundamental data such as thermodynamic and transport properties play essential roles, and often highly accurate thermodynamic properties have to be known. In the past 10 years, worldwide efforts have continued to collect accurate experimental data for such fundamental properties of these HFC compounds. Now reliable equations of state have been developed based on a large amount of experimental property data. No doubt, these studies would provide great assistance to scientists and engineers engaged in the fields of air-conditioning, heat-pumps, and refrigeration. Also, they contribute significantly to our scientific knowledge, since in the past only a few compounds have been studied in such detail. It is a great opportunity to check the validity of theoretical models against the experimental data, and vice versa.

In this paper, we focus on the ideal-gas heat capacity and virial coefficients, since they can be calculated from theoretical models based on intramolecular energies and intermolecular potential functions. First, the ideal-gas heat capacity and, then, the virial coefficients are examined. The compounds investigated are R-23, R-32, R-125, R-134a, R-143a, and R-152a.

2. IDEAL-GAS HEAT CAPACITY

The isobaric (C_p^0) and isochoric (C_v^0) heat capacities in the ideal-gas state are related by $C_p^0 = C_v^0 + R$. $C_p^0(T)$ can be obtained experimentally by extrapolating speed-of-sound data or $C_p(T)$ data from flow calorimeter experiments to the zero-pressure limit. Theoretically, C_v^0 is calculated from molecular energies and can be written as

$$C_v^0 = \tfrac{3}{2}R + C_i \tag{1}$$

The first term arises from the translational freedom of the center of mass in a molecule and the second term, C_i, is the contribution from the internal degrees of freedom through a molecular partition function, $z(T)$:

$$C_i = R\frac{\partial}{\partial T}\left(T^2\frac{\partial \ln z(T)}{\partial T}\right) \tag{2}$$

$$z(T) = \sum_n d_n \exp\left(-\frac{\varepsilon_n}{kT}\right) \tag{3}$$

where ε_n is an internal energy in a molecule with a quantum number n, and d_n is the degeneracy of this energy state. The molecular internal energy results from four kinds of internal degrees of freedom: electronic states, nuclear states of constituent atoms, overall molecular rotation, and vibrational states. These four states cannot be regarded as being completely independent; e.g., couplings exist between nuclear spin and molecular rotation, electronic and vibrational states, and vibrational and rotational states. The situation depends strongly upon the type of molecule and the temperature range of interest. For the present compounds and temperature range of our interest (say, 100 to 1000 K), the states may be safely separated, and the correction due to such couplings can be applied if necessary. The contributions from electronic and nuclear states and any couplings due to these states can be ignored for the present case. Then we have only contributions to C_i from rotations and vibrations. The vibrational and/or rotational energy levels are determined experimentally by molecular spectroscopy. However, accurate and complete analyses of the spectroscopic data are prohibitively complicated as the number of atoms in a molecule increases. So far, sufficiently accurate information is limited to a few simple molecules such as diatomic and triatomic molecules. Therefore, for general polyatomic molecules, one commonly adopts a drastically simplified approximation to calculate C_i: the so-called rigid-rotator harmonic-oscillator (RRHO) model. Fortunately, this simple model provides C_v^0 (or C_p^0) with a fair accuracy (within a couple of percent) in the moderate temperature range (100 to 1000 K), if the harmonic or fundamental vibrational frequencies are known correctly. For molecules with a large molar mass such as those investigated in the present study and for temperatures above about 100 K, a quantum rigid rotor can safely be treated as a classical rigid rotor, and then the contribution to C_i is $3R/2$ for all nonlinear polyatomic molecules. Previous investigators (Rodgers et al. [1] and Chase et al. [2]) adopted this RRHO model to calculate C_p^0 for R-23 and R-32. In the present study, we have investigated some corrections, δC, to the RRHO model due to the vibrational anharmonicites and/or vibration–rotation couplings for these molecules, based on a method developed by Pennington and Kobe [3]. Then the sum of all contributions to C_p^0 (or $C_p^0 = C_v^0 + R$) can be expressed by

$$C_p^0 = 4R + C_{HO} + \delta C \tag{4}$$

$$C_{HO} = R\left(\frac{hc}{kT}\right)^2 \sum_i \frac{d_i v_i^2 \exp(-hcv_i/kT)}{[1-\exp(-hcv_i/kT)]^2} \tag{5}$$

As for the ethane-derivative HFC compounds, R-125, R-134a, R-143a, and R-152a, the RRHO model cannot simply be applied. This is because they have a special internal degree of freedom—internal rotation—which R-23 and R-32 do not possess. It is a motion peculiar to the C_i contribution. At very low temperatures, it acts like a harmonic oscillator with a low-amplitude torsional vibration of the two methyl-type groups around the C–C axis, and at very high temperatures the methyl-type groups rotate freely against each other. At the high-temperature limit, if it is a harmonic oscillator, it contributes to C_i by R, while if it is a free rotor, its contribution is $R/2$. Therefore, the internal rotation must be treated separately and calculated in a special way. Equation (4) becomes

$$C_p^0 = 4R + C_{HO}(\text{without torsional mode}) + C(\text{internal rotation}) + \delta C \tag{6}$$

Since its first discovery as a heat capacity anomaly on ethane, many works have investigated the internal rotation both experimentally and theoretically. The standard theoretical method is to treat it as an independent degree of freedom: a rotating top on the rigid frame under a periodic potential field, without any couplings with the overall molecular rotations and internal vibrational modes. The periodic potential is assumed in the first order approximation by

$$V = \tfrac{1}{2} V_n(1 - \cos n\theta) \tag{7}$$

where θ is the torsional angle between the two tops, and $n = 3$ is assumed for most of the cases. V_3 is often called a barrier height of the internal rotation. Chen et al. [4] used this model for the internal rotation to calculate C_p^0 for R-125, R-134a, R-143a, and R-152a, with the use of the RRHO model for other degrees of freedom. In their calculations, the energy levels of the internal rotation with the periodic potential were calculated by solving eigenvalues of the proper Hamiltonian matrix up to 15,000 cm^{-1}. We have used the values tabulated by Pitzer and Gwinn [5] to check their calculations by the use of numerical interpolation of the table and found both to agree within 0.1%. Therefore, we adopt the interpolation method of Pitzer and Gwinn's table as being sufficiently accurate for the present study.

Although the internal rotation causes the complications described in the C_i calculation for these compounds, more serious problems arise for

large polyatomic molecules as studied here, that is, the spectroscopic assignment of fundamental frequencies. The correct assignment is never simple and straightforward for these compounds, and the major contribution to C_i comes from the proper fundamental frequencies. In fact, before talking about internal rotation, vibrational anharmonicities, and vibration–rotation couplings, the correct fundamental frequencies must be known properly. Therefore, our discussion is somewhat involved.

In the following sections, we discuss each individual compound separately in detail and compare the present theoretical calculations with experimental data as well as with previous theoretical works. The final results of all molecules of present interest are summarized in Table VII and Fig. 8.

2.1. R-23 (Trifluoromethane)

The molecular symmetry of this molecule belongs to the C_{3v} point group, and the fundamental vibrational frequencies are three totally symmetric A_1 modes plus three doubly degenerated E modes. The vibrational and rotational energy, ε_{VR}, referred to the lowest (ground vibrational) state, can be written in the following general form:

$$\varepsilon_{VR} = \sum_i (v_i + X_{ii} + g_{ii}) n_i + \sum_i \sum_{j \geq i} X_{ij} n_i n_j + \sum_i \sum_{j \geq i} g_{ij} l_i l_j + F_v \qquad (8)$$

where v_i is the fundamental frequency, n_i is the vibrational quantum number, l_i is the quantum number of vibrational angular momenta arising from degenerated vibrational modes, X_{ij} ($=X_{ji}$) and g_{ij} ($=g_{ji}$) are anharmonicity constants, and the term F_v stands for the rotational level at the n_i vibrational state and contains vibration–rotation coupling constants. If we ignore the vibration–rotation coupling and anharmonicities ($X_{ij}=0$ and $g_{ij}=0$), Eq.(8) becomes the RRHO model. The vibrational contribution to C_p^0 is given by Eq. (5) through Eqs. (2) and (3). Chase et al. [2] applied such a model for this molecule, by the use of fundamental frequencies reported by Long et al. [6]. Since Kirk and Wilt [7] obtained anharmonicity constants (X_{ij}) as well as new fundamentals, which are corrected for Fermi resonance, we have adopted their values and made new calculations for this molecule, taking into account the vibrational anhamonicity correction to the RRHO model. The present fundamental frequencies are compared with those used by Chase et al. in Table I, and the anharmonicity constants are shown in Table II. The slightly different frequencies did not cause significant errors in this molecule, while the anharmonicity effect on C_p^0 results in a difference of up to 2% at 1000 K. This is shown in Fig. 1.

Table I. Fundamental Frequencies (cm^{-1}) for R-23

Mode	Approx. description	Chase et al. [2]	This study
ν_1 (A_1)	C–H stretching	3035	2991.1
ν_2 (A_1)	C–F stretching	1137	1141.3
ν_3 (A_1)	FCF bending	700	700.1
ν_4 (E)	CF_3 stretching	1376	1377.7
ν_5 (E)	CF deformation	1152	1158.4
ν_6 (E)	CF_3 rocking	508	507.8

Table II. Anharmonicity Constants (cm^{-1}) [7] for R-23

X_{11}	−3.6	X_{23}	−1.6	X_{36}	0.0
X_{12}	−5.7	X_{24}	−1.1	X_{44}	−0.5
X_{13}	4.8	X_{25}	−5.6	X_{45}	−13.7
X_{14}	−5.1	X_{26}	−1.6	X_{46}	−1.0
X_{15}	−7.9	X_{33}	−2.4	X_{55}	0.65
X_{16}	−0.6	X_{34}	−0.8	X_{56}	−7.8
X_{22}	−0.75	X_{35}	−5.7	X_{66}	−0.4

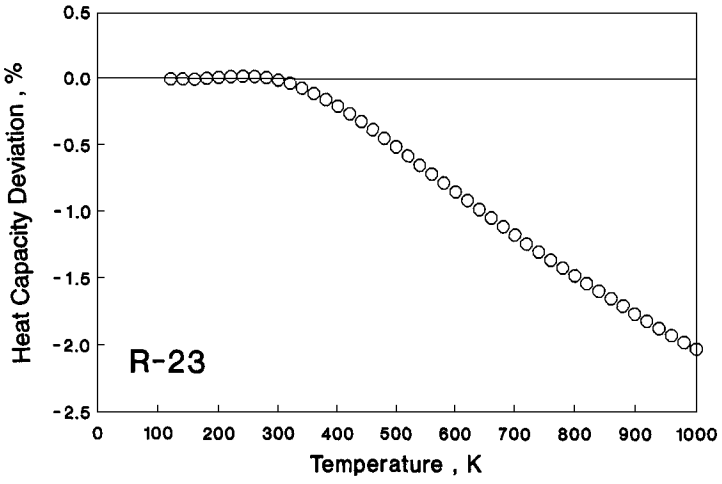

Fig. 1. Ideal-gas heat capacity of R-23: deviation plot relative to this study. (○) Chase et al. [2].

2.2. R-32 (Difluoromethane)

This molecule with C_{2v} point-group symmetry has nine fundamentals and no degenerated frequencies: four A_1 modes, one A_2 mode, two B_1 modes, and two B_2 modes. Previous investigators (Chase et al. [2] and Rodgers et al. [1]) used the RRHO model to calculate C_p^0. Recently, Tillner-Roth and Yokozeki [8] have made new calculations including the corrections due to the vibrational anharmonicity and rotation–vibration coupling effects, and the details are given in their paper. C_p^0 values of Chase et al. are compared with these new calculations in Fig. 2. The anharmonicity effect is clearly seen and is very similar to the case of R-23 (see Fig. 1). Experimental C_p^0 values of Hozumi et al. [9] agree with the new calculations within 0.12%.

2.3. R-125 (Pentafluoroethane)

The molecular symmetry of R-125 is C_s, and it has 11 A′-mode and 7 A″-mode fundamental frequencies. Gas-phase infrared and Raman spectra and a liquid-phase infrared spectrum were observed by Nielsen et al. [10], and low-frequency bands were examined by Kinumaki and Kozuka [11] and by Brown et al. [12]. In their C_p^0 calculations, Chen et al. [4] selected 10 higher fundamental frequencies from the values of Nielsen et al. [10] and the remaining lower fundamental frequencies of Kinumaki and Kozuka [11] and Brown et al. [12]. Later, modified vibrational assignments for this molecule were proposed by Compton and Rayner

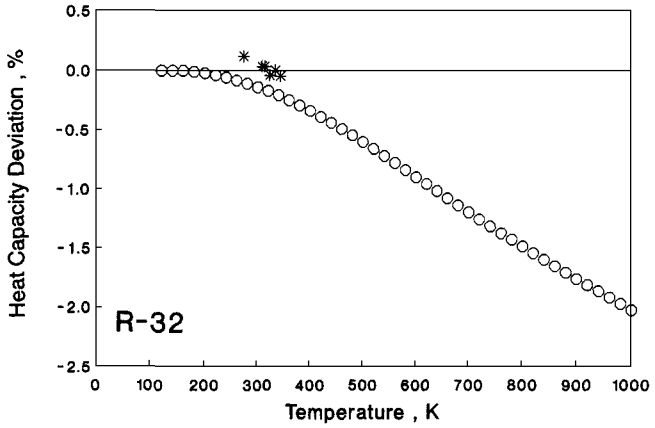

Fig. 2. Ideal-gas heat capacity of R-32: deviation plot relative to this study. (○) Chase et al. [2]; (*) Hozumi et al. [9].

[13], based on their analysis of vibrational spectra of CF_3–CF_2I and similar compounds. These two sets of assignments are shown in the third and fourth columns in Table III. They chose a new fundamental of 654 cm^{-1} from the values observed by Nielsen et al., removing 508 cm^{-1} of the Chen et al. [4] selection, and the torsional fundamental of 74 cm^{-1} (Brown et al. [12]) was adopted instead of 82 cm^{-1} (Kinumaki and Kozuka [11]). In addition, three mode (symmetry) assignments of the selected fundamentals (1309, 1198, and 578 cm^{-1}) were interchanged ($A' \leftrightarrow A''$). Such mode assignment changes do not affect the C_p^0 calculation for this molecule, since no degenerate frequencies with C_s symmetry are present. If the molecule had a higher symmetry and degenerate frequencies, the mode (symmetry) assignments would be important and greatly affect the C_p^0 calculation, since the degeneracy factor must be multiplied in the C_p^0 contribution for each degenerated frequency. The proper "selection" of fundamental frequencies is our only concern here and the mode "assignment" is irrelevant, except for the torsional-mode assignment. Chen and coworkers' selection of 82 cm^{-1} from studies by Kinumaki and Kozuka [11] is more convincing for the torsional mode. The torsional frequency,

Table III. Fundamental Frequencies (cm^{-1}) for R-125

Mode	Approx. description	Chen et al. [4]	Compton & Rayner [13]	This study[a]
ν_1 (A′)	C–H stretching	3008	3008	3008 (n)
ν_2 (A′)	CCH bending	1393	1393	1447 (n)
ν_3 (A′)	CF_3 sym. stretching	1309	1218	1359 (n)
ν_4 (A′)	CF_3 sym. stretching	1218	1198	1218 (n)
ν_5 (A′)	CF_2 sym. stretching	1111	1111	1145 (n)
ν_6 (A′)	C–C stretching	867	867	867 (n)
ν_7 (A′)	CF_3 sym. deformation	725	725	725 (n)
ν_8 (A′)	CF_2 bending	577	654	573 (n)
ν_9 (A′)	CF_3 asym. deformation	523	523	525 (n)
ν_{10} (A′)	CF_2 wagging	361	361	361 (b)
ν_{11} (A′)	CF_3 rocking	246	217	217 (b)
ν_{12} (A″)	CCH deformation	1359	1359	1359 (n)
ν_{13} (A″)	CF_3 asym. stretching	1198	1309	1309 (n)
ν_{14} (A″)	CF_2 asym. stretching	1145	1145	1198 (n)
ν_{15} (A″)	CF_3 asym. deformation	508	577	577 (b)
ν_{16} (A″)	CF_2 twisting	413	413	413 (b)
ν_{17} (A″)	CF_3 rocking	216	247	246 (k)
ν_{18} (A″)	Torsion	82	72	82 (k)

[a] b, k, and n indicate frequencies observed by Brown et al. [12], Kinumaki and Kozuka [11], and Nielsen et al. [10], respectively; the reasons for the present selection are given in the text.

however, does not contribute to C_p^0 directly, except for the barrier estimation, since the torsional mode is treated as an internal rotation in the present model as mentioned earlier.

It appears that the C_p^0 values for R-125 in the TRC tables [14] are based on Compton and Rayner's fundamentals [13], with the barrier height and the reduced moment of inertia for the internal rotation similar to those used by Chen et al. [4]. Our calculations have reproduced practically the same values as in the TRC tables, using these fundamentals and the internal rotation parameters, and also significantly improved the C_p^0 values previously calculated by Chen et al. [4] with respect to the experimental values of Gillis [15] and Hozumi et al. [16]. Discrepancies of more than 2% between the earlier calculated values and the experimental values have now become within about 0.5 and 1% for the Gillis and the Hozumi et al. data, respectively (see Fig. 3). Although the modified fundamental assignment improved the theoretical C_p^0 values, significant discrepancies between them still exist, indicating some incorrect fundamentals. This led us to reexamine the earlier papers on the infrared and Raman spectra of this molecule.

As mentioned before, the important difference between Chen and coworkers' [4] and Compton and Rayner's [13] choices in the fundamentals is *508 cm^{-1} (the former) or 654 cm^{-1} (the latter). Replacing 508 cm^{-1}* with something else may be justified, since this weak IR absorption band was adopted tentatively by Nielsen et al. [10]. However, the choice of 654 cm^{-1} is questionable. It was a weak infrared band, not observed in the

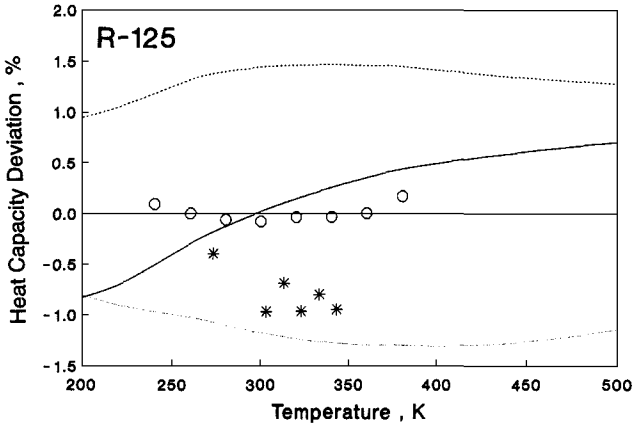

Fig. 3. Ideal-gas heat capacity of R-125: deviation plot relative to this study. (——) TRC [14]; (----) Chen et al. [4]; (····) RRHO (see text); (*) Hozumi et al. [9]; (○) Gillis [15].

Raman spectrum by Nielsen et al. [10], who actually interpreted it as a combination band of the two observed fundamentals (248- and 414-cm^{-1} bands), and their interpretation is quite reasonable. Obviously, Compton and Rayner [13] searched absorption bands between 550 and 700 cm^{-1} in the IR spectra of Nielsen et al., to find the CF_2 deformation mode based on their comparative analyses of CF_3–CF_2X (X = I, Br, or Cl) compounds. There exists only a strong IR absorption band around 577 cm^{-1} (573–587 cm^{-1}), as well as strong Raman bands around 578 cm^{-1}, but it was already assigned as one of the fundamentals (A″ CF_3 deformation mode). Therefore, they picked up the weak band at 654 cm^{-1}, regardless of the assignment of this band by Nielsen et al. It is very likely that two fundamental modes (the corresponding CF_2 and CF_3 deformations) overlap in the 578-cm^{-1} region. Thus, we chose the strong absorption at 573 cm^{-1} as a new fundamental for the CF_2 deformation mode, instead of the 508- or 654-cm^{-1} band. In addition to their tentative assignment of 508 cm^{-1}, Nielsen et al. [10] discussed the uncertain assignments of two A′ fundamentals (1111 and 1393 cm^{-1}), with an alternative selection of 1447 cm^{-1}, and 1111 and 1393 cm^{-1} were tentatively assumed to be fundamentals. In this molecule, the second highest frequency in the A′ modes must come from the C–H deformation, the characteristic frequency of which is about 1460 cm^{-1}. We select the alternative frequency of 1447 cm^{-1} as a new fundamental, replacing 1393 cm^{-1}, which can be interpreted as a combination band of the two fundamentals ($525 + 867 = 1392\ cm^{-1}$). Similarly, the tentative frequency of 1111 cm^{-1} is interpreted as a combination band of the two fundamentals ($246 + 867 = 1113\ cm^{-1}$) and can be replaced by 1145 cm^{-1}, which was already selected as a fundamental. Now we need another fundamental. The CF_3 asymmetric stretching frequencies (A′ mode) of n-C_3F_7I and n-C_3F_7 are reported to be 1328 and 1354 cm^{-1}, respectively [13]. In the present molecule, ν_{12} (1359 cm^{-1}), which is assigned as the A″ CCH bending mode, is very close to such frequencies and then could overlap the ν_3 (CF_3 symmetric stretching-mode) band. Therefore, we choose 1359 cm^{-1} as the ν_3 fundamental as well, and our complete vibrational assignments of this molecule are listed in the last column in Table III.

Concerning the internal rotation, the barrier height V_3 and the reduced moment of inertia Ir for the top rotation from Chen and coworkers' [4] work are sufficiently accurate and are acceptable for the present study. We have adopted their values of 18.150 $kJ \cdot mol^{-1}$ (or 1517 cm^{-1}) for V_3 and 55.278 $g \cdot cm^2$ for Ir. With these internal rotation parameters and our newly assigned vibrational fundamentals, the C_p^0 values of this molecule have been calculated, and the results are compared with the experimental C_p^0 values as well as other theoretically calculated

values in Fig. 3. For the purpose of curiosity, the rigid-rotor harmonic oscillator (RRHO) calculation, which treats the torsional motion as an harmonic oscillator with an infinitestimal vibration with the torsional frequency, just like other fundamental modes, is also shown in Fig. 3. The RRHO model calculation shows the magnitude of the contribution from the internal rotation effect; in the region of 200–500 K, the internal rotation contributes 0.8 to 1.3% to C_p^0 with respect to the RRHO, with a maximum contribution at about 400 K in this molecule. The previous theoretical calculations by Chen et al. [4] are higher by 1–1.5% in this temperature range than the present result, while the TRC table values [14], which are based on Compton and Rayner's fundamentals [13], differ by −0.8% at low temperatures and by +0.7% at high temperatures with respect to the present result. The experimental data of Gillis [15] are in remarkable agreement with our calculated values; deviations are less than 0.1% except for one point at the highest temperature (0.17%). It is striking proof that the present simple model is sufficiently accurate for the C_p^0 calculation, provided that the experimental data are correct. Unfortunately, the experimental data of Hozumi et al. [16] deviate by −0.4 to −1.0% from the present result. To resolve this discrepancy, several attempts have been made by changing fundamentals and the internal rotation parameters. Hozumi and co-workers' data [16] could be reproduced only within 0.3% by a set of parameters consisting of significantly modified fundamentals and the use of one third of the present barrier height of the internal rotation. It may be argued that the present model is too simple to deal with molecule as complicated as R-125, with various possible vibrational and/or rotational anharmonities and Fermi resonance. However, such anharmonicity effects are not so large in the temperature range 200–400 K (experimental range), and also, at least the experimental data of Gillis [15] are consistent with the present results.

2.4. R-134a (1,1,1,2-Tetrafluoroethane)

The molecular symmetry belongs to the C_s point group, but due to twovery close principal moments of inertia, it can be regarded as an accidental symmetric top; this molecule should have 11 A′-mode and 7 A″-mode fundamental frequencies. There were large disparities both in the selection and in the mode assignment of fundamental frequencies between Edgell et al. [17] and Nielsen and Halley [18]. Chen et al. [4] made an extensive survey of vibrational modes for halogenated methanes and ethanes and selected their own fundamentals for this molecule from the observed IR spectra of Edgell et al. [17] and Nielsen and Halley [18]. Two low frequencies, 225 and 120 cm^{-1}, were taken from Danti and

Wood's [19] far-infrared spectrum. With the torsional mode of 120 cm^{-1}, they estimated the internal rotation barrier of 18.527 $kJ \cdot mol^{-1}$ (1548.7 cm^{-1}) and then calculated the ideal-gas heat capacity. As pointed out by Goodwin and Moldover [20] and Hozumi et al. [21], the calculated values of Chen et al. [4] were about 2% higher than their accurate ($\pm 0.2\%$) experimental C_p^0, derived from their speed-of-sound measurements. It seems that there are some incorrect frequency assignments in the Chen et al. selection of the fundamentals. Goodwin and Moldover [20] also compared their C_p^0 with the calculations of Basu and Wilson [22], which were based on the RRHO model with fundamental assignments by Harnish and Hirschman [23], and found the calculated values to be even worse. This may be due to the simple RRHO approximation, by neglecting the internal rotation, and/or due to the incorrect fundamental selection. To determine the reason, we have calculated the C_p^0 values using the fundamentals of Harnish and Hirschman [23] both with the RRHO model and with the internal rotation model, in which the internal rotation barrier has been tested from 15 up to 19 $kJ \cdot mol^{-1}$. We were unable to reproduce the C_p^0 values obtained by Basu and Wilson [22]; there seem to be some miscalculations and/or misprints in their paper. When we use the Harnish and Hirschman fundamentals [23] with the parameters of Chen et al. for the internal rotation [4], the C_p^0 values are not worse than those of Chen et al. [4], but instead some improvements have been observed with respect to the experimental values; the 2% errors mentioned above reduce to about 1%. Their fundamental assignments seem to be improved, but there are still some problems. They picked up the completely new frequency of 1070 cm^{-1} as a fundamental and removed the previously selected fundamental of 1374 cm^{-1}. Their ν_{13} (A″) value of 1463 cm^{-1} is too high, because this mode should correspond to the asymmetric stretching of the CF_3 group, and in R-23 it is 1377 cm^{-1}. Therefore, we recover 1374 cm^{-1} and assign it as ν_{13}, which is the choice of Edgell et al. [17] and Chen et al. [4], and remove the 1070 cm^{-1} as well as the 1296 (ν_3) cm^{-1}, which was used twice as ν_{14}, of Harnish and Hisrchman [23]. The 1463 cm^{-1} now belongs to the A′ group, like the choice of Chen et al. [4]. Our preferred selection and assignment of fundamentals are shown in Table IV, in comparison with previous works. As for the torsional mode, we adopt the value of 111 cm^{-1} recommended by Brier [24], which is comfortably in accord with that observed by Harnish and Hirschman [23]. This gives a barrier height V_3 of 15.272 $kJ \cdot mol^{-1}$ (1276.6 cm^{-1}) for the internal rotation with the reduced moment of inertia of 24.77×10^{-40} $g \cdot cm^2$; the corresponding values used by Chen et al. [4] were 18.527 $kJ \cdot mol^{-1}$ (1548.7 cm^{-1}) and 26.06×10^{-40} $g \cdot cm^{-1}$, respectively.

Table IV. Fundamental Frequencies (cm^{-1}) for R-134a

Mode	Nielsen et al. [18]	Edgell et al. [17]	Chen et al. [4]	Harnish et al. [23]	This study
ν_1 (A′)	2984	2984	2984	2986	2986
ν_2 (A′)	1464	1431	1464	1427	1464
ν_3 (A′)	1427	1296	1427	1296	1427
ν_4 (A′)	1298	1096	1298	1186	1296
ν_5 (A′)	1103	1067	1103	1103	1186
ν_6 (A′)	973	908	973	1070	1103
ν_7 (A′)	843	844	842	846	846
ν_8 (A′)	665	666	665	666	666
ν_9 (A′)	549	550	549	557	557
ν_{10} (A′)	408	358	408	410	410
ν_{11} (A′)	225	201	225	222	222
ν_{12} (A″)	3013	3015	3013	3015	3015
ν_{13} (A″)	1182	1374	1374	1463	1374
ν_{14} (A″)	665	1189	1182	1296	1296
ν_{15} (A″)	539	972	885	971	971
ν_{16} (A″)	352	541	539	542	542
ν_{17} (A″)	225	407	352	358	358
ν_{18} (A″)[a]	—	124	120	112	111

[a] Torsional mode.

With the present choice of fundamentals and internal rotation parameters, the C_p^0 values of this molecule have been calculated and are compared in Fig. 4 with the values of Chen et al. [4], as well as several experimental data in the literature. Data derived from the speed-of-sound measurements of Goodwin and Moldover [20] and of Hozumi et al. [21] agree with the present result within their experimental errors (<0.2%). Other speed-of-sound data of Beckermann and Kohler [25] and flow calorimetric data of Tuerk et al. [26] are also in good agreement with the present calculation. The speed-of-sound data of Zhu et al. [27] obviously scatter too much, but they agree within two times their estimated standard deviation (0.51%). The theoretical values of Chen et al. [4] are about 1 to 2% larger than the present result over the temperatures 200–500 K.

2.5. R-143a (1,1,1-Trifluoroethane)

This molecule has the point-group symmetry of C_{3v}, and the normal vibrations divide into symmetry species in the following manner: five A_1 (totally symmetric) modes plus one A_2 (antisymmetric with respect to the

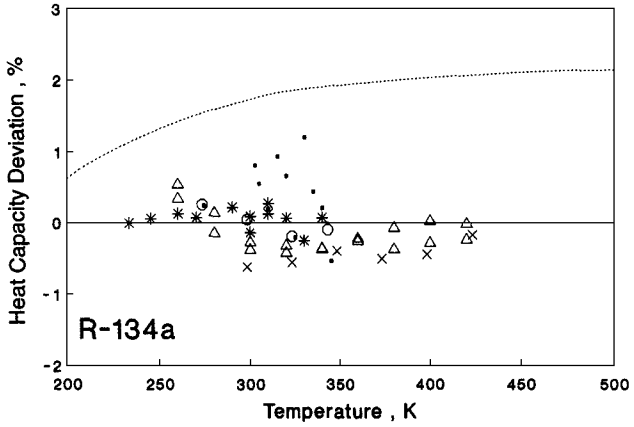

Fig. 4. Ideal-gas heat capacity of R-134a: deviation plot relative to this study. (----) Chen et al. [4]; (*) Goodwin and Moldover [20]; (○) Hozumi et al. [21]; (△) Beckermann and Kohler [25]; (×) Tuerk et al. [26]; (•) Zhu et al. [27].

planes of symmetry) mode plus six E (degenerate) modes. The torsional oscillation belongs to the A_2 symmetry and is inactive both in the infared and in the Raman spectra in the gas and liquid phases, while the A_1 and E (degenerated) species are active in both cases. There was wide divergence among the fundamental assignments proposed by several researchers before 1950. However, Nielsen et al. [28] made fairly convincing assignments for the fundamentals, except for the torsional frequency of 238 cm^{-1} (estimated from their observed combination bands), which was later observed at 220 cm^{-1} in the solid phase by Durig et al. [29]. In the gas phase, a torsional mode of 220 ± 10 cm^{-1} was also observed with the neutron inelastic scattering measurements of Brier [24]. To calculate the ideal-gas thermodynamic properties including C_p^0, Chen et al. [4] adopted the fundamentals proposed by Nielsen et al. [28], except for the torsional mode of 238 cm^{-1}; the torsional frequency of 220 cm^{-1} was used for estimating their internal rotation barrier of 3167 $cal \cdot mol^{-1}$ (13.251 $kJ \cdot mol^{-1}$, or 1108 cm^{-1}). More recently, however, precise values for the rotational constants and the internal-rotation barrier height of 1093 cm^{-1} (13.075 $kJ \cdot mol^{-1}$) have been determined by Meerts and Ozier [30], as well as the reduced moment of inertia of 5.144×10^{-40} $g \cdot cm^{-1}$ for the internal rotation. We have recalculated C_p^0 for this molecule with these new constants and the same fundamentals as selected by Chen's et al. [4] and found that the differences between the calculations of Chen et al. [4] and ours are very minor, as shown in Fig. 5, where C_p^0 values of Gillis [15]

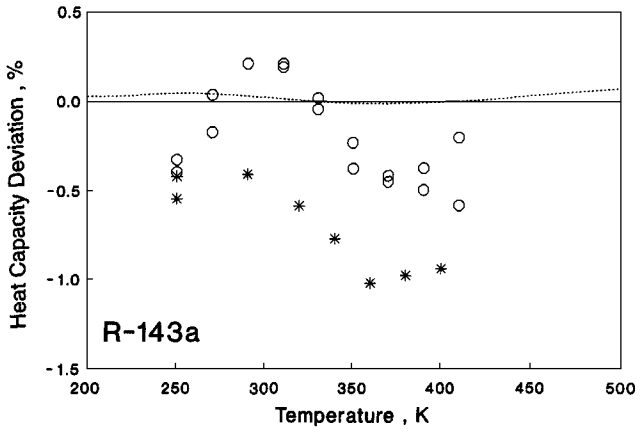

Fig. 5. Ideal-gas heat capacity of R-143a: deviation plot relative to this study. Model 1. (----) Chen et al. [4]; (*) Gillis [15]; (○) Beckermann and Kohler [25].

and Beckermann and Kohler [25] experimentally determined from speed-of-sound measurements are also compared with the present calculation. The C_p^0 values in TRC tables [31] for this molecule are essentially the same as those in the calculations of Chen et al. [4], and thus they are not shown in Fig. 5. While the data of Beckermann and Kohler [25] agree fairly well with the calculated values (within about $\pm 0.5\%$), those of Gillis [15] are systematically lower by about 0.5–1.0% than the theoretical ones. This is rather disturbing, since the former data are based on a mixture sample of R-143a (99.3%) and something (0.7%) which has a peak very close to the main peak in their gas chromatography, while the latter data are based on practically pure R-143a (99.99%), and both samples seem to have been free of air and water. It appears that the data of Gillis [15] are more reliable for the C_p^0 of this molecule. This indicates that there are some problems either with the fundamental assignments or with the assumptions used in the theoretical model.

We have carefully reexamined the earlier papers on infrared and Raman spectra by Cowan et al. [32], Nielsen et al. [28], and Hatcher and Yost [33] but arrived at the same fundamentals as selected by Chen et al. [4] in Table V, although there are peculiarities in some of the fundamental bands; the strongest infrared band, at 1233 cm^{-1} (ν_9), was not observed in the Raman spectrum by Hatcher and Yost [33]; the ν_2 fundamental at 1408 cm^{-1} (strong IR band) was not observed in the Raman spectrum either, and the band center (Q branch) of the ν_{10} fundamental (970 cm^{-1}) split into two or three peaks. Recently, Fraser et al. [34] made precise

Table V. Fundamental Frequencies (cm^{-1}) for R-143a

Mode	Approx. description	This study and Chen et al. [4]
ν_1 (A_1)	C–H stretching	2975
ν_2 (A_1)	CH_3 deformation	1408
ν_3 (A_1)	C–F stretching	1280
ν_4 (A_1)	C–C stretching	830
ν_5 (A_1)	CF_3 deformation	602
ν_6 (A_2)	Torsion	220
ν_7 (E)	C–H stretching	3035
ν_8 (E)	CH_3 deformation	1443
ν_9 (E)	C–F stretching	1233
ν_{10} (E)	CH_3 rocking	970
ν_{11} (E)	CF_3 deformation	541
ν_{12} (E)	CF_3 rocking	365

studies on the 970-cm^{-1} band with an electric-resonance optothermal spectrometer and microwave-side band CO_2 laser and found strong Fermi resonance between the ν_{10} fundamental and the combination bands of $2\nu_6+\nu_{11}$ and $\nu_5+\nu_{12}$, creating three states (peaks) at about 970 cm^{-1}. The 970-cm^{-1} fundamental is not a pure state but is a mixed state of nearly equal admixtures of ν_{10} and $\nu_5+\nu_{12}$. They expect that these strong interacting vibrations will persist at high excitation energies such as $2\nu_6+\nu_{11}+n\nu_i$, $\nu_{10}+n\nu_i$, $\nu_5+\nu_{12}+n\nu_i$, and $3\nu_6+\nu_{12}+n\nu_i$. It seems that there are many Fermi resonances (accidental resonances) in this molecule. This may be related in part to the fact that this symmetric-top molecule is almost an accidentally (highly degenerated) spherical top, with nearly equal rotational constants of A and B: $(A-B)/B=6\%$ [34]. Fermi resonance, however, should not cause too many problems for the C_p^0 calculation, since the energy level due to such resonance usually splits into high and low levels by a nearly equal amount; the higher-frequency contribution to the C_p^0 tends to cancel the lower-frequency one. Another complication in this molecule may arise due to the degenerated vibrational modes with C_{3v} symmetry and an accidentally spherical top. The anharmonicity arising from the vibrational angular momenta [see Eq. (8)] might be responsible for the present discrepancy in C_p^0 between the theory and the experiment. Such effects, however, will be much smaller in the present temperature region. Therefore, we suspect that the traditional theoretical model of the internal rotation may be applied for this molecule. The model assumes that the internal rotation is independent of and decoupled from any other internal modes. However, Fraser et al. [34] have clearly observed that the

strong v_6 (torsional-mode) couplings with other internal vibrational modes exist, as mentioned above. The theoretical formulation for such coupled motions is possible in principle but would be quite complicated and require much more detailed information on the coupling strength from the spectroscopic experiment.

In this circumstance, we propose a phenomenological model to calculate C_p^0 arising from the coupled/anharmonic internal rotation. We calculate C_p^0 with the RRHO model with the fundamentals in Table V except for the torsional mode, and the torsional mode is assumed to be a completely free (or nearly free) internal rotation with no rotational barrier. If any excitation process such as a rotational barrier with extra couplings exists, it will show up as an excess heat capacity. Thus, any such extra excitation process in the heat capacity may be ascribed to a Schottky-type anomaly, C_{Sch} [35]:

$$C_{\text{Sch}} = R\left(\frac{\Delta E}{kT}\right)^2 \frac{\exp(\Delta E/kT)}{[1+\exp(\Delta E/kT)]^2} \tag{9}$$

where ΔE is the characteristic excitation energy of the process in question. Then Eq. (6) can be expressed as

$$C_p^0 = 4R + C_{\text{HO}}(\text{without torsional mode}) + (0.5+\delta)\,R + C_{\text{Sch}} \tag{10}$$

The third term is the contribution from the free ($\delta = 0$) or nearly free ($\delta > 0$) rotation. With the characteristic excitation energy, ΔE of 510 cm^{-1} and δ of 0.092, the calculated values agree with the experimental C_p^0 data of Gillis [15] within about 0.2%; the results are shown in Fig. 6 as Model 2. The situation shown in Fig. 5 has now been significantly improved for the data of Gillis.

2.6. R-152a (1,1-Difluoroethane)

With the molecular symmetry of C_s, this molecule has 11 A′-mode and 7 A″-mode fundamental frequencies. The infrared and Raman spectra of its vapor and liquid were observed by Smith et al. [36], except for the torsional mode. Chen et al. [4] selected their fundamentals and the torsional frequency of 222 cm^{-1}, which had been observed by Fateley and Miller [37], to calculate C_p^0. The barrier height of 13.45 $\text{kJ}\cdot\text{mol}^{-1}$ (1125 cm^{-1}) and the reduced moment of inertia of 5.129×10^{-40} $\text{g}\cdot\text{cm}^2$ for the internal rotation were used in the C_p^0 calculations. The TRC tables (Rodgers [38]) adopted the calculations of Chen et al. [4], and later the TRC tables (Chao and Rodgers [14]) revised the C_p^0 calculations without any detailed

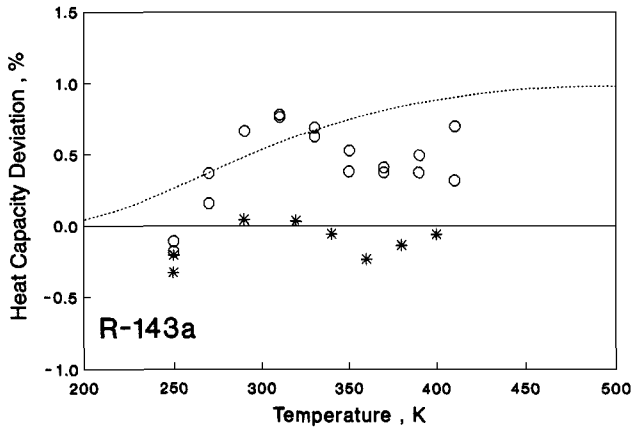

Fig. 6. Ideal-gas heat capacity of R-143a: deviation plot relative to this study. Model 2. (----) Chen et al. [4]; (*) Gillis [15]; (○) Beckermann and Kohler [25].

description. We have compared the experimental data of Gillis [15], Beckermann and Kohler. [25], Hozumi et al. [39], and Tuerk et al. [26] with those of Chen et al. [4] and the TRC tables (Chao and Rodgers [14]). The revised TRC table [14] values are about 1.2% larger than the experimental values of Gillis [15], Hozumi et al. [39], and Tuerk et al. [26] and, also, about 0.8% larger than the values calculated by Chen et al. [4]. The values of Chen et al. [4] are clearly better than the revised TRC values [14], and agree with Beckermann and Kohler's [25] data within about $\pm 0.5\%$, but are systematically larger than the other experimental data by more than 0.5%. It seems that the data of Beckermann and Kohler [25] contain some systematic errors, since all the other experimental data (speed-of-sound experiments obtained by Gillis [15] and Hozumi et al. [39] and flow-calorimetric experiments by Tuerk et al. [26]) are in a good agreement, within about $\pm 0.3\%$. This may be due partially to the fact that the purity of the sample used by Beckermann and Kohler [25] is the lowest (99.7%) among these researchers'.

Recently, revised parameters for the internal rotation have been determined by Villamanan et al. [40], namely, a barrier height of 13.90 kJ · mol^{-1} (1163 cm^{-1}) and a reduced moment of inertia of 5.022×10^{-40} g · cm^2. The reduced moment of inertia of 5.022×10^{-40} g · cm^2 was not reported in their paper, but in the present study it was calculated with their values of a methyl-top moment of inertia of 5.329×10^{-40} g · cm^{-1}, an angle of 18.48° between the symmetry axis of the methyl group and the *a*-principal axis, and principal moments of inertia of 88.41×10^{-40} g · cm^2

for I_A and 162.5×10^{-40} g·cm^2 for I_C. With these revised parameters for the internal rotation, we have calculated C_p^0 using the same fundamentals as selected by Chen et al. [4], listed in Table VI. The use of these new parameters for the internal rotation has not significantly improved the situation; the differences between Chen and co-workers' [4] and our calculations are less than 0.2%. This suggests that there are incorrect fundamental frequencies in the selection, which were taken from the fundamental assignment made by Smith et al. [36]. In the present study, we have examined ab initio molecular orbital (MO) calculations. Villamanan et al. [40] calculated the ab initio force constants and normal vibrational frequencies. Since they used the force constants without any scaling, these frequencies correspond to the zero-order harmonic frequencies, which are generally much higher than the fundamental frequencies. To estimate the fundamentals, we have used an empirical correlation; the amount of correction is proportional to the squares of the frequency, which roughly hold for simple molecules: $\Delta\nu = -\beta\nu^2$. The proportionality constant, β, of 1.5×10^{-5} cm for the C–H stretching modes and that of 2.1×10^{-5} cm for the rest of the modes are adopted, respectively. The ab initio zero-order frequencies and the estimated fundamentals are shown in

Table VI. Fundamental Frequencies (cm^{-1}) for R-152a

Mode	Approx. description	Ab initio[a]	Chen et al. [4]	This study
ν_1 (A′)	C–H stretching	3207.1	3018	3053
ν_2 (A′)	C–H stretching	3149.6	2978	3001
ν_3 (A′)	C–H stretching	3102.7	2960	2958
ν_4 (A′)	CCH deformation	1506.9	1460	1459
ν_5 (A′)	CCH deformation	1471.2	1414	1426
ν_6 (A′)	CCH deformation	1410.5	1372	1369
ν_7 (A′)	CCH deformation	1184.7	1143	1155
ν_8 (A′)	CF_2 stretching	1177.8	1129	1149
ν_9 (A′)	C–C stretching	892.8	868	876
ν_{10} (A′)	CF_2 bending	576.9	571	570
ν_{11} (A′)	CF_2 wagging	475.5	470	471
ν_{12} (A″)	C–H *a*-stretching	3204.8	3001	3051
ν_{13} (A″)	CH_3 deformation	1508.8	1460	1461
ν_{14} (A″)	CH_2 deformation	1440.9	1360	1397
ν_{15} (A″)	CF_2 *a*-stretching	1188.8	1171	1159
ν_{16} (A″)	CH_3 rocking	978.6	930	958
ν_{17} (A″)	CF_2 twisting	389.3	383	386
ν_{18} (A″)	Torsion	257.6	222	(256)[b]

[a] Ab Initio MO calculations of Villamanan et al. [40].
[b] This frequency was not used; see the text.

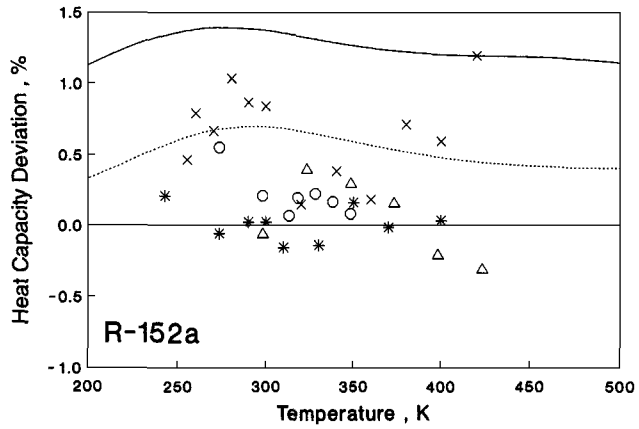

Fig. 7. Ideal-gas heat capacity of R-152a: deviation plot relative to this study. (----) Chen et al. [4]; (——) TRC [31]; (*) Gillis [15]; (×) Beckermann and Kohler [25]; (○) Hozumi et al. [39]; (△) Tuerk et al. [26].

Table VI. The torsional frequency of 256 cm^{-1} seems high, but this does not concern us, since it is not used for C_p^0 calculations; the torsional mode is treated separately as the internal rotation.

Using the present fundamentals and the internal rotation parameters mentioned above, we have calculated the C_p^0 of R-152a, and the results are compared with various available experimental and theoretical values in

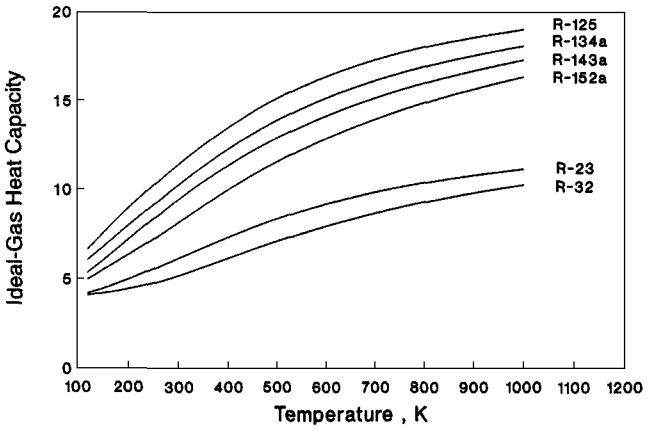

Fig. 8. Nondimensionalized ideal-gas heat capacity (C_p^0/R) of R-23, R-32, R-125, R-134a, R-143a, and R-152a, calculated in this study.

Table VII. Nondimensionalized Ideal-Gas Heat Capacity (C_p^0/R) Calculated in This Study

T (K)	R-23	R-32	R-125	R-134a	R-143a	R-152a
120	4.186	4.072	6.657	6.055	5.341	4.963
140	4.340	4.135	7.243	6.531	5.771	5.297
160	4.528	4.213	7.820	7.011	6.238	5.638
180	4.736	4.306	8.381	7.490	6.718	5.983
200	4.958	4.414	8.925	7.965	7.196	6.334
220	5.189	4.538	9.451	8.428	7.666	6.689
240	5.427	4.677	9.961	8.893	8.125	7.049
260	5.670	4.832	10.450	9.351	8.572	7.414
280	5.916	5.001	10.932	9.802	9.007	7.784
300	6.162	5.181	11.399	10.244	9.429	8.156
320	6.408	5.370	11.851	10.674	9.839	8.529
340	6.651	5.566	12.287	11.095	10.235	8.900
360	6.890	5.766	12.706	11.502	10.618	9.265
380	7.124	5.968	13.107	11.894	10.987	9.623
400	7.352	6.170	13.493	12.270	11.342	9.972
420	7.572	6.371	13.860	12.630	11.683	10.312
440	7.785	6.569	14.209	12.973	12.009	10.642
460	7.990	6.763	14.539	13.300	12.322	10.960
480	8.187	6.952	14.852	13.611	12.622	11.268
500	8.375	7.137	15.148	13.906	12.908	11.564
520	8.555	7.317	15.427	14.187	13.182	11.849
540	8.728	7.492	15.690	14.454	13.444	12.124
560	8.892	7.661	15.939	14.708	13.695	12.388
580	9.050	7.825	16.173	14.949	13.935	12.643
600	9.200	7.983	16.394	15.177	14.165	12.888
620	9.344	8.136	16.603	15.395	14.386	13.123
640	9.481	8.284	16.800	15.602	14.597	13.350
660	9.611	8.428	16.986	15.799	14.800	13.569
680	9.737	8.566	17.162	15.986	14.994	13.776
700	9.856	8.700	17.328	16.165	15.182	13.980
720	9.971	8.829	17.485	16.335	15.361	14.176
740	10.080	8.954	17.634	16.492	15.534	14.367
760	10.185	9.075	17.775	16.648	15.701	14.550
780	10.286	9.192	17.909	16.796	15.861	14.728
800	10.382	9.306	18.036	16.938	16.016	14.901
820	10.475	9.415	18.156	17.075	16.165	15.067
840	10.564	9.521	18.270	17.205	16.309	15.229
860	10.649	9.624	18.379	17.330	16.448	15.385
880	10.731	9.724	18.478	17.451	16.582	15.536
900	10.810	9.820	18.576	17.566	16.711	15.683
920	10.886	9.914	18.670	17.677	16.836	15.825
940	10.959	10.005	18.760	17.783	16.957	15.963
960	11.029	10.093	18.845	17.886	17.074	16.097
980	11.097	10.178	18.927	17.984	17.187	16.227
1000	11.163	10.261	19.005	18.079	17.297	16.352

Fig. 7. Except for one odd point, the experimental data of Hozumi et al. [39], Gillis [15], and Tuerk et al. [26] are all in good agreement with the present calculations, within about 0.25%. The data of Beckermann and Kolher [25] scatter around the values calculated by Chen et al. [4]. The revised TRC table values [14] appear much too large.

Finally, the nondimensionalized ideal-gas heat capacities (C_p^0/R) calculated in the present study are summarized in Table VII for R-23, R-32, R-125, R-134a, R-143a, and R-152a and are also plotted in Fig. 8.

3. VIRIAL COEFFICIENTS

Many efforts have been made to determine the virial coefficients in the past, both experimentally and theoretically. The virial coefficients, particularly the second (B) and third (C) coefficients, are of special interest. At moderate and low pressures, the three-term (B and C) virial equation of state and the ideal-gas heat capacity data are sufficiently accurate to represent all thermodynamic properties. More significantly, they provide a critical bridge between experiment and theory. The virial coefficients are directly related to the intermolecular potential among molecules. The Lennard–Jones (12,6) potential has been widely used in theoretical work, and it provides sufficiently accurate representations of real nonpolar fluid properties, e.g., the second virial coefficient and also the transport properties (thermal conductivity and viscosity) [41]. Among other empirical potential functions, the square well-type potential has an attractive nature, although it is unrealistic. It gives us analytically simple closed forms for the virial coefficients B and C [42] and serves as a convenient tool to correlate the experimental virial coefficients. However, neither the Lennard–Jones nor the square-well potential can represent experimental virial coefficients for polar molecules satisfactorily. Yet some researchers adopt the square-well potential function for their experimental analyses to correlate the data, by abandoning the concept of the potential function and by treating it as a convenient and arbitrary fitting function, e.g., fitting the B and C coefficients employing different sets of arbitrary parameters for the "potential" function. In this case, there is no physical significance for the parameters, and the potential function, although it is unrealistic, is no longer the potential function—it is "simply" an empirical fitting function; it is very difficult to justify whether it represents the proper temperature dependence of the virial coefficients, particularly outside the experimental data range, as well as the temperature derivatives.

For polar compounds, extra contributions due to the asymmetric charge distribution in a molecule arise in the interaction potential, and the first-order term is the permanent electric dipole–dipole interaction.

Stockmayer [43] proposed dipole–dipole interaction terms in addition to the Lennard–Jones nonpolar potential for the second virial coefficients of polar molecules. This treats a gas as an ensemble of spherical molecules whose intermolecular potential has a repulsive term proportional to r^{-12}, an attractive term proportional to r^{-6}, and point-dipoles at their center. This potential function has been applied successfully for correlating the second virial coefficients of various polar molecules [41]. Rowlinson [44] first calculated the third virial coefficient using this potential and examined the third virial coefficients of ammonia and water and, later, various other polar compounds. Except for water, in which higher multipole interactions may be needed, the second and third virial coefficients of polar gases were consistently explained with numerically fair accuracy, in comparison to the relatively large experimental uncertainties of the data. It must be remembered that the experimental viral coefficients are difficult quantities to obtain accurately and often contain large uncertainties and/or systematic errors due to the improper truncation of virial equations of state.

Recently, accurate thermodynamic properties including the virial coefficients have been measured for various HFC compounds, thanks to the worldwide effort on alternative refrigerant research. These are highly polar compounds, and some of them posses even larger dipole moments than ammonia and water do. This presents a great opportunity to examine the virial coefficients with the Stockmayer potential.

3.1. Theoretical Model

The Stockmayer potential, u_{ij}, between the ith and the jth molecules is given as

$$u_{ij} = 4\varepsilon_{ij}\left[\left(\frac{\sigma}{r}\right)_{ij}^{12} - \left(\frac{\sigma}{r}\right)_{ij}^{6}\right] - \frac{\mu_i \mu_j}{r_{ij}^3} g(\theta_i, \theta_j, \phi_{ij}) \tag{11}$$

$$g(\theta_i, \theta_j, \phi_{ij}) = 2\cos\theta_i \cos\theta_j - \sin\theta_i \sin\theta_j \cos\phi_{ij} \tag{12}$$

Here θ_i is the angle of the ith dipole $\vec{\mu}_i$ with the vector, $\vec{r}_i - \vec{r}_j$, and ϕ_{ij} is the azimuthal angle between the planes containing $\vec{\mu}_i$ and $\vec{r}_i - \vec{r}_j$, and $\vec{\mu}_j$ and $\vec{r}_i - \vec{r}_j$.

The formulae for the second (B) and third (C) virial coefficients for angle-dependent potentials are given as follows [41]:

$$B = -\frac{N}{32\pi^2 V} \iint f_{12}\, d\vec{q}_1\, d\vec{q}_2 \tag{13}$$

$$C = -\frac{N^2}{192\pi^3 V} \iiint f_{12} f_{13} f_{23}\, d\vec{q}_1\, d\vec{q}_2\, d\vec{q}_3 \tag{14}$$

with

$$d\vec{q}_i = \frac{1}{4\pi} dx_i\, dy_i\, dz_i \sin\theta_i\, d\theta_i\, d\phi_{ij} \tag{15}$$

$$f_{ij} = \exp(-u_{ij}/kT) - 1 \tag{16}$$

where the pairwise additivity is assumed for the three body interaction potential in C.

The second virial coefficient can be integrated analytically for the Stockmayer potential, when the exponential term is expanded in an infinite series.

$$B = b_0 \left(\frac{4}{T^*}\right)^{1/4} \left[\Gamma\left(\frac{3}{4}\right) - \frac{1}{4} \sum_{n=1}^{\infty} \sum_{l=0}^{n/2} \frac{2^n G_l}{n!} \binom{n}{2l} \times \Gamma\left(\frac{2n-2l-1}{4}\right) t^{*2l} T^{*(n+l)/2} \right] \tag{17}$$

$$G_l = \frac{1}{1+2l} \sum_{m=0}^{l} \binom{l}{m} \frac{3^m}{1+2m} \tag{18}$$

with two dimensionless parameters, T^* and t^*, and hard-sphere molar volume, b_0:

$$T^* = kT/\varepsilon_{ij} \tag{19}$$

$$t^* = \frac{\mu_i \mu_j}{2\sqrt{2}\, {}_{ij}\sigma_{ij}^3} \tag{20}$$

$$b_0 = 2\pi N \sigma_{ij}^3/3 \tag{21}$$

Although the summation with the n index goes to infinity, for practical purposes it is sufficiently accurate (well below 0.1% errors for B values) with a limited number in n of 35, even for low T^* of 0.7 and high t^* of 1.4. For the molecules studied in the present case, it can be valid at temperatures down to below the triple point.

The third virial coefficient integral may be calculated by a method similar to that used for the second virial coefficient. However, in this case the expansion coefficients are not just γ functions, but contain complicated and tedious integrals of the mutual orientations and distances of three interacting molecules. Rowlinson [44] showed that the integral can be

separated into two parts: the nonpolar (Lennard–Jones) and polar (dipole–dipole) contributions. The nonpolar part was calculated by Kihara [45] and Bird et al. [46] and expressed by

$$C = b_0^2 \sum_{j=0}^{\infty} c(j)\, T^{*-(j+1)/2} \tag{22}$$

Kihara's [47] values of $c(j)$ with j up to 17 are used in the present work. The polar contribution to the virial C coefficient, ΔC, is given by Rowlinson [44]:

$$\Delta C = \frac{3}{2} b_0^2 \sum_{n=2}^{\infty} \sum_{m=2}^{n} \frac{2^n}{n!} \binom{n}{m} \frac{t^{*m}}{T^{*(n/2-m/4-1/2)}} Q_{n,m} \tag{23}$$

$Q_{n,m}$ is the complicated eightfold integral of mutual orientations and distances among the three molecules. Rowlinson [44] has calculated the $Q_{n,m}$ terms up to $n = 16$ and $m = 8$. We have adopted his tabulated values for $Q_{n,m}$, extrapolating m up to 16. Our calculations for C values have reproduced the calculations of Rowlinson with sufficient accuracy. When the temperatures are high enough, the convergence of the infinite sum is rapid. However, it becomes very slow as the temperature decreases. In the present limited summation, the accuracy of C values is poor near and below the temperature at the C maximum; the calculated values should be regarded as being semiquantitative at those temperatures, where the experimental data contain large uncertainties as well. Nonetheless, both virial coefficients, B and C, are expressed by analytical functions of the three parameters, T^*, t^* (dimensionless), and b_0 (molar volume units), which are functions of the molecular constants—molecular diameter (σ), dipole moment (μ), and potential energy depth (ε)—for each pure compound. The temperature derivatives of B and C can easily be derived and calculated from the above analytical equations.

3.2. Analysis and Results

There are many ways to determine the potential constants from the experimentally reduced virial coefficients. The traditional method is that used by Rowlinson and others [41]. It uses the experimentally known dipole moment, and then only the experimental second virial coefficient, B, and the dB/dT (slope) of a pure compound at some specified temperature

are needed. The corresponding theoretical expressions are equated as follows:

$$\frac{TB_{\text{obs}}}{3229.818\mu_{\text{obs}}^2} = \frac{T^*(B/b_0)_{\text{th}}}{t^*} \tag{24}$$

$$\frac{T(dB_{\text{obs}}/dT)}{B_{\text{obs}}} = \frac{T^*(dB_{\text{th}}/dT^*)}{B_{\text{th}}} \tag{25}$$

The numerical constant of 3229.818 is due to the unit conversion factor, where B and b_0 are in $\text{cm}^3 \cdot \text{mol}^{-1}$, T in Kelvin, and μ in Debye. These two simultaneous equations are solved numerically for the two unknowns T^* and t^* and by the two-dimensional Newton–Raphson method. Then b_0 can be simply obtained from

$$b_0 = \frac{B_{\text{obs}}}{(B/b_0)_{\text{th}}} \tag{26}$$

The numerical solution of these two nonlinear equations behaves quite well, and the roots are easily obtained. However, the solution often depends upon the specified temperature. Experimental $B(T)$ and dB/dT at one specified temperature give one solution, while at another specified temperature they give another solution. There is a way to improve the fit and to obtain more definitive potential constants for the present potential function. This traditional method assumes the dipole strength to be the actual value of the experimental molecular dipole moment, regardless of the effective nature in the model potential: a point dipole at the center of the spherical molecule. The actual charge distribution differs considerably from that of a point-dipole. It should be regarded as the effective dipole moment, just as σ (molecular diameter) is the effective spherical size of the actual nonspherical molecule, and therefore we treat it as an adjustable parameter to be determined from the experimental virial coefficients. If the potential function is physically meaningful at all, these effective parameters derived from the experimental virial coefficients should be in physically reasonable and acceptable ranges of the parameters.

A couple of alternative methods have been examined to determine the potential constants to fit the experimental B nearly perfectly and definitively. One of the methods is to use the B values and the slopes (dB/dT) at two specified temperatures, that is, to use two equations of Eq. (25) to get t^* and T^* and to use Eq. (26) to get b_0. Another method is to use three B values without the slope information at three specified temperatures (T_1, T_2, and T_3) using the following relation. Neither method

fixes the dipole moment, which is simply calculated from the determined T^*, t^*, and b_0 through Eqs. (19)–(21).

$$[B(T_1)/B(T_2)]_{obs} = [B(T_1)/B(T_2)]_{th} \tag{27}$$

$$[B(T_3)/B(T_2)]_{obs} = [B(T_3)/B(T_2)]_{th} \tag{28}$$

$$b_0 = \frac{1}{3}\left[\frac{B(T_1)_{obs}}{\{B(T_1)/b_0\}_{th}} + \frac{B(T_2)_{obs}}{\{B(T_2)/b_0\}_{th}} + \frac{B(T_3)_{obs}}{\{B(T_3)/b_0\}_{th}}\right] \tag{29}$$

Both of these methods are able to reproduce experimental B values nearly perfectly including all other B values at unused temperatures; no regression analysis is needed. To demonstrate this, we have used the second virial coefficients of R-134a of Goodwin and Moldover [20]. For their entire data range of 233 to 423 K [acoustic second virial coefficients, $\beta_a(T)$, plus Weber's [55] $B(T)$ values], our results show a standard deviation of 0.9 $cm^3 \cdot mol^{-1}$, from the data at 245, 310, and 400 K only; the percentage deviation is 0.15%. This may be compared with their regression fits using the square-well potential function form; the standard deviation of the fit was 1.5 $cm^3 \cdot mol^{-1}$. The potential parameters in the present results are 170.46 K, 0.4593 nm, and 2.946 Debye for the energy well depth, molecular diameter, and dipole strength, respectively. These parameters are not physically absurd and may be regarded reasonable as the effective quantities. Another comment may be worthy of mention here regarding their analyses, using the Stockmayer potential. In their paper, Goodwin and Moldover [20] state, "We attempted to fit the appropriate expressions resulting from the (m, 6, 3) Stockmayer potential function to fit the $\beta_a(T)$ data and the $B(T)$ data. Very poor fits were obtained with $9 \leqslant m \leqslant 60$." $m = 12$ corresponds to the case in the present study. This is completely contradictory to our present conclusion. It is, however, quite likely that the method of their analysis is based on the traditional method, mentioned above, using a fixed value of the known molecular dipole moment. One data point with the fixed dipole moment would not fit all data well, as discussed earlier. The dipole moment strength is an effective value in the Stockmayer potential model and cannot be equated precisely to the actual molecular dipole moment, which is certainly not a point-dipole located at the center of a spherical molecule.

Although the present method can present the experimental second virial coefficient precisely, the third virial coefficient could not be represented well by the use of the potential constants determined from the second virial coefficient. This is due in part to the inaccuracy of the experimental data and, possibly, to the incompleteness of the assumed potential form. Higher-order terms such as dipole–quadruple interactions may be needed

in addition to the Stockmayer potential, as well as the correction terms due to the nonspherical geometry of molecules and due to the pairwise additivity assumption to the three-body interaction potential. To test theoretical potential forms, however, highly accurate experimental data are required over a wide range of temperatures, and typical experimental uncertainties in $B(T)$ amount to a couple of percent or more, which would be insufficient to judge the theory. Furthermore, the second virial coefficient is relatively insensitive to the detailed shape of the potential energy function, while the third virial coefficient contains more information about the potential function. Although the experimental uncertainties in $C(T)$ are larger, the potential constants can be determined from the $C(T)$ data alone, using equations similar to Eqs. (27)–(29) for the C expressions. However, in this case $B(T)$ data were unable to be represented satisfactorily with these constants.

In the present study, an effort has been made to reconcile both $B(T)$ and $C(T)$. A set of molecular constants $(\varepsilon, \sigma, \mu)$ has been determined so as to fit the overall experimental $B(T)$ data, generally within 2 or 3%, instead of fitting experimental $B(T)$ data too faithfully, but to represent the $C(T)$ data as well. The results for R-23, R-32, R-125, R-134a, R-143a, and R-152a are shown in Table VIII. The second and third virial coefficients thus calculated are tabulated in Tables IX and X, respectively. These parameters are not necessarily the best possible sets of values, since no regression-type analyses have been made, but with these potential constants, both $B(T)$ and $C(T)$ data are consistently presented for these polar compounds. The present theoretical results for these compounds are shown in Tables IX and X and compared with experimental values reported in the literature in Figs. 9–20. From these figures, it may be said that the present model potential is capable of reproducing both the experimental second and the experimental third virial coefficients for the present polar molecules with a fair accuracy, although

Table VIII. Molecular Potential Constants for Several HFC Compounds

Compound	t^*	ε/k (K)	b_0 ($cm^3 \cdot mol^{-1}$)	$\sigma \times 10^{10}$ (m)	μ (Debye)[a]
R-152a	1.007	256.27	74.595	3.896	2.433
R-143a	1.100	220.00	76.000	3.920	2.386
R-134a	0.935	272.17	69.410	3.803	2.334
R-125	0.900	251.50	68.800	3.792	2.195
R-32	1.163	210.00	57.236	3.567	2.080
R-23	0.900	216.00	51.200	3.437	1.756

[a] 1 Debye $= \frac{1}{3} \times 10^{-29}$ C · m.

Table IX. Second Virial Coefficients ($cm^3 \cdot mol^{-1}$) Calculated with the Stockmayer Potential

T (K)	R-23	R-32	R-125	R-134a	R-143a	R-152a
200	−541.8	−1074.3	−1205.2	−1842.1	−1434.6	−1958.9
210	−468.0	−894.5	−1016.1	−1514.0	−1196.4	−1606.9
220	−409.4	−758.3	−870.8	−1269.7	−1015.6	−1345.2
230	−361.7	−652.4	−756.4	−1082.8	−874.8	−1145.4
240	−322.5	−568.3	−664.6	−936.6	−763.0	−989.2
250	−289.6	−500.4	−589.6	−819.8	−672.5	−864.7
260	−261.8	−444.5	−527.5	−724.9	−598.0	−763.7
270	−238.0	−398.0	−475.3	−646.7	−535.9	−680.5
280	−217.4	−358.8	−431.0	−581.3	−483.5	−610.9
290	−199.5	−325.3	−393.0	−525.9	−438.8	−552.2
310	−169.7	−271.4	−331.3	−437.9	−366.8	−458.8
320	−157.3	−249.5	−306.0	−402.4	−337.4	−421.2
330	−146.2	−230.2	−283.5	−371.2	−311.6	−388.2
340	−136.2	−213.1	−263.6	−343.8	−288.6	−359.1
350	−127.1	−197.8	−245.7	−319.4	−268.1	−333.3
360	−118.9	−184.0	−229.5	−297.5	−249.7	−310.3
370	−111.4	−171.7	−214.9	−278.0	−233.1	−289.6
380	−104.6	−160.5	−201.7	−260.3	−218.0	−270.9
390	−98.3	−150.3	−189.6	−244.3	−204.4	−254.0
400	−92.5	−141.0	−178.6	−229.7	−191.9	−238.6
410	−87.1	−132.5	−168.4	−216.4	−180.5	−224.6
420	−82.2	−124.7	−159.1	−204.2	−170.0	−211.8
430	−77.6	−117.5	−150.4	−193.0	−160.3	−199.9
440	−73.3	−110.8	−142.4	−182.6	−151.3	−189.0
450	−69.3	−104.7	−135.0	−173.1	−143.0	−179.0
460	−65.6	−98.9	−128.1	−164.2	−135.3	−169.6
470	−62.1	−93.6	−121.6	−156.0	−128.1	−161.0
480	−58.8	−88.6	−115.6	−148.3	−121.4	−152.9
490	−55.7	−84.0	−109.9	−141.1	−115.2	−145.3
500	−52.8	−79.6	−104.6	−134.4	−109.3	−138.3
510	−50.1	−75.5	−99.6	−128.1	−103.8	−131.7
520	−47.5	−71.7	−94.9	−122.2	−98.6	−125.5
530	−45.0	−68.1	−90.5	−116.7	−93.8	−119.7
540	−42.7	−64.7	−86.3	−111.4	−89.2	−114.2
550	−40.5	−61.5	−82.3	−106.5	−84.8	−109.0

we have clearly observed that the *best* potential constants for $B(T)$ and *those* for $C(T)$ are inconsistent, as mentioned above.

The next task is to examine whether these effective potential constants are physically meaningful and reasonable. The molecular diameter may be estimated from the van der Waals atomic radii: 0.77 (C), 0.56 (F), and 0.23 (H), in 10^{-10} m units. The longest interatomic distance in the molecule can be taken as the diameter of the spherical body. Thus, the diameters for

Table X. Third Virial Coefficients ($L^2 \cdot mol^{-2}$) Calculated with the Stockmayer Potential

T (K)	R-23	R-32	R-125	R-134a	R-143a	R-152a
230	0.0115	—	—	—	—	—
240	0.0142	0.0030	−0.0193	—	−0.0047	—
250	0.0152	0.0160	0.0023	—	0.0207	—
260	0.0153	0.0229	0.0149	—	0.0346	—
270	0.0149	0.0262	0.0220	−0.0075	0.0416	0.0049
280	0.0143	0.0273	0.0258	0.0092	0.0445	0.0212
290	0.0135	0.0271	0.0274	0.0193	0.0450	0.0306
300	0.0126	0.0262	0.0277	0.0251	0.0440	0.0356
310	0.0118	0.0250	0.0273	0.0283	0.0423	0.0380
320	0.0110	0.0236	0.0264	0.0297	0.0401	0.0386
330	0.0102	0.0221	0.0253	0.0300	0.0378	0.0381
340	0.0095	0.0207	0.0240	0.0295	0.0355	0.0370
350	0.0089	0.0193	0.0227	0.0287	0.0332	0.0355
360	0.0083	0.0180	0.0214	0.0276	0.0310	0.0338
370	0.0077	0.0168	0.0201	0.0263	0.0290	0.0321
380	0.0073	0.0156	0.0190	0.0250	0.0271	0.0303
390	0.0068	0.0146	0.0178	0.0237	0.0253	0.0286
400	0.0064	0.0136	0.0168	0.0225	0.0237	0.0270
410	0.0060	0.0128	0.0158	0.0213	0.0222	0.0254
420	0.0057	0.0120	0.0149	0.0201	0.0208	0.0240
430	0.0053	0.0112	0.0141	0.0190	0.0195	0.0226
440	0.0051	0.0106	0.0133	0.0180	0.0184	0.0213
450	0.0048	0.0099	0.0126	0.0170	0.0173	0.0201
460	0.0046	0.0094	0.0119	0.0161	0.0163	0.0190
470	0.0043	0.0088	0.0113	0.0152	0.0154	0.0180
480	0.0041	0.0084	0.0107	0.0144	0.0146	0.0170
490	0.0039	0.0079	0.0102	0.0137	0.0139	0.0161
500	0.0038	0.0075	0.0097	0.0130	0.0132	0.0153
510	0.0036	0.0072	0.0092	0.0124	0.0125	0.0146
520	0.0034	0.0068	0.0088	0.0118	0.0119	0.0139
530	0.0033	0.0065	0.0084	0.0113	0.0114	0.0132
540	0.0032	0.0062	0.0081	0.0108	0.0108	0.0126
550	0.0031	0.0059	0.0077	0.0103	0.0104	0.0120
560	0.0029	0.0057	0.0074	0.0098	0.0099	0.0115
570	0.0028	0.0054	0.0071	0.0094	0.0095	0.0110
580	0.0027	0.0052	0.0068	0.0090	0.0091	0.0105
590	0.0027	0.0050	0.0066	0.0087	0.0088	0.0101
600	0.0026	0.0048	0.0063	0.0083	0.0084	0.0097

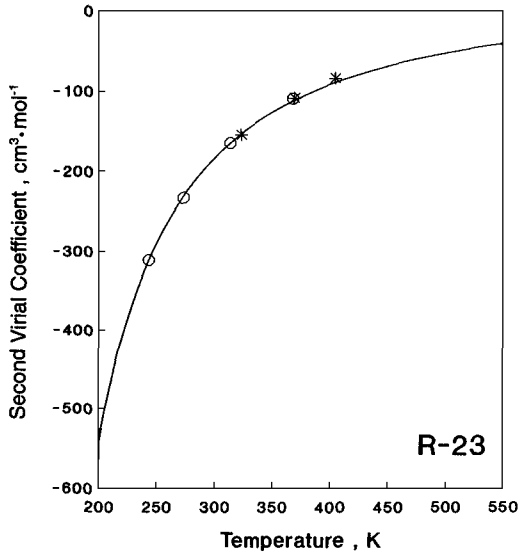

Fig. 9. The second virial coefficients of R-23. (——) This study; (∗) Sutter and Cole [50]; (○) Lange and Stein [51].

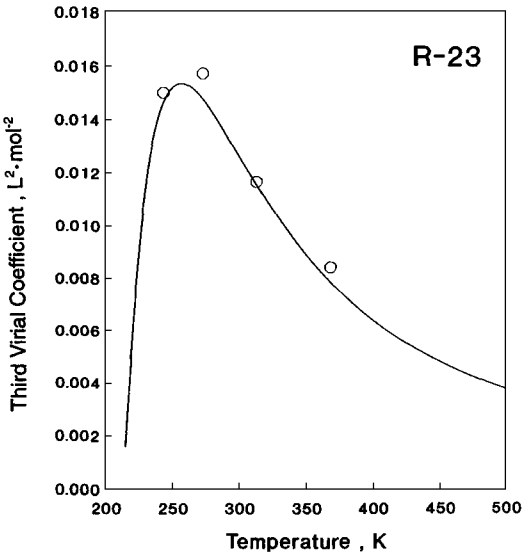

Fig. 10. The third virial coefficients of R-23. (——) This study; (○) Lange and Stein [51].

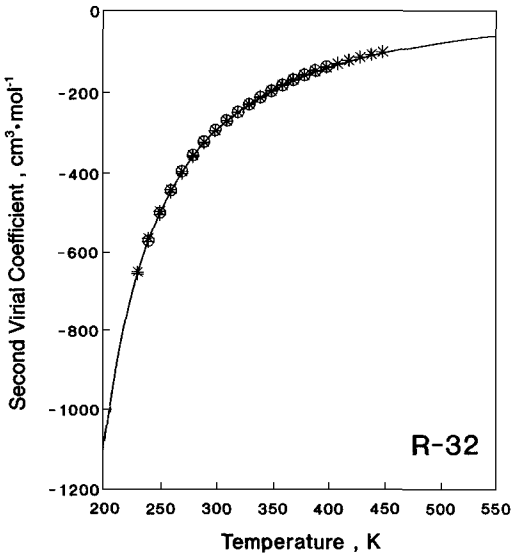

Fig. 11. The second virial coefficients of R-32. (——) This study; (*) de Vries [52]; (○) Defibaugh et al. [54]; (+) Hozumi [53].

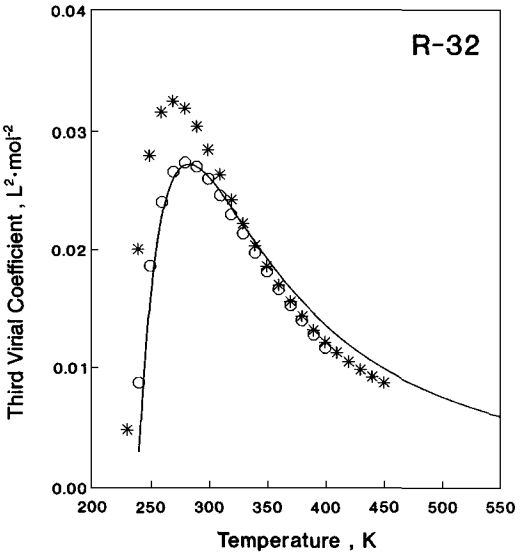

Fig. 12. The third virial coefficients of R-32. (——) This study; (*) de Vries [52]; (○) Defibaugh et al. [54].

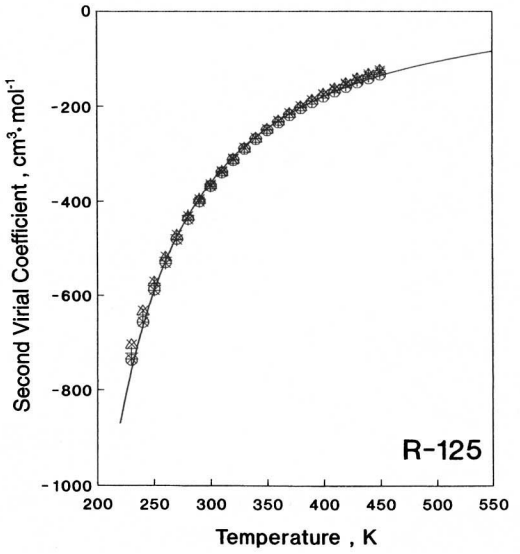

Fig. 13. The second virial coefficients of R-125. (——) This study; (*) Zhang [56]; (○) Hozumi [53]; (+) de Vries [52]; (△) Weber [55]; (×) Gillis [15].

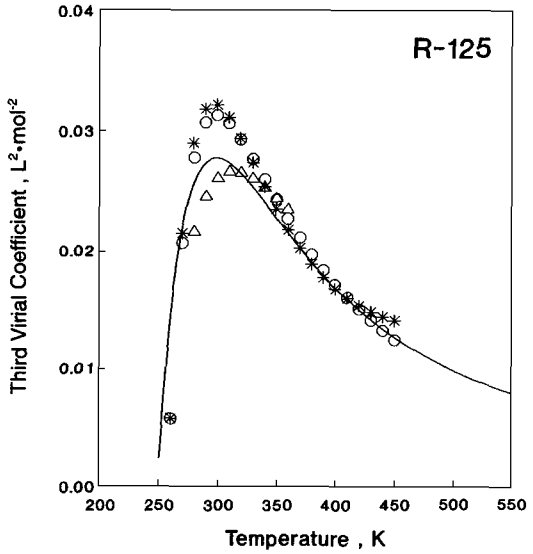

Fig. 14. The third virial coefficients of R-125. (——) This study; (*) Gillis [15]; (○) Zhang [56]; (△) Boyes and Weber [57].

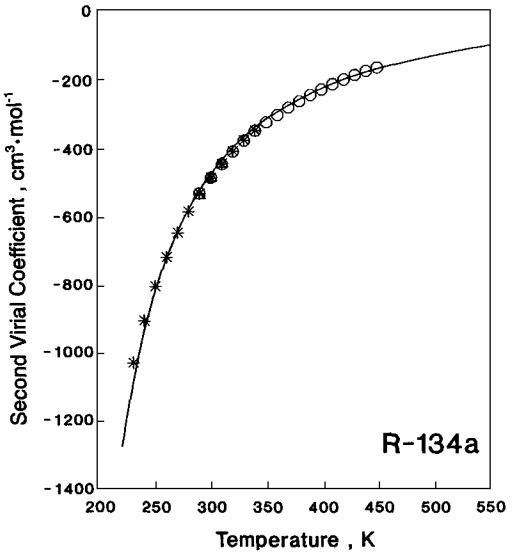

Fig. 15. The second virial coefficients of R-134a. (——) This study; (○) Tillner-Roth and Baehr [59]; (∗) Goodwin and Moldover [20]; (△) Bignell and Dunlop [58].

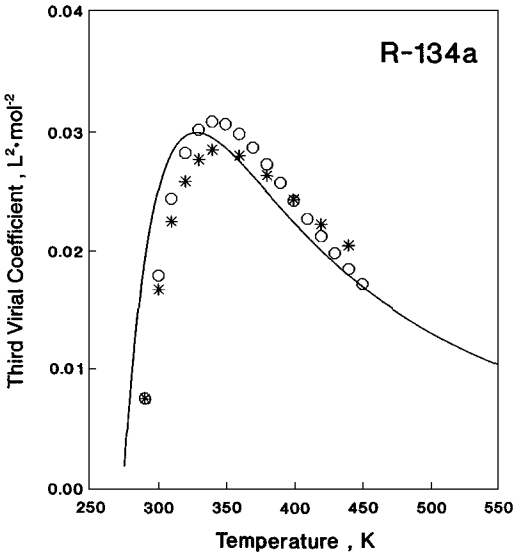

Fig. 16. The third virial coefficients of R-134a. (——) This study; (○) Tillner-Roth and Baehr [59]; (∗) Goodwin and Moldover [20].

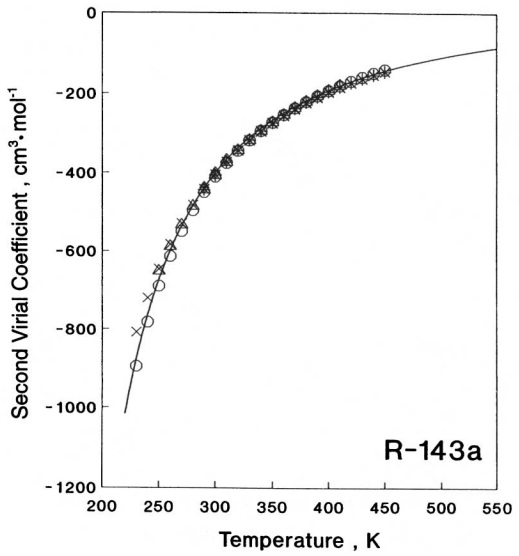

Fig. 17. The second virial coefficients of R-143a. (——) This study; (*) Zhang [56]; (○) Weber [55]; (×) Gillis [15]; (△) Beckermann and Kohler [25]; (◇) Bignell and Dunlop [58].

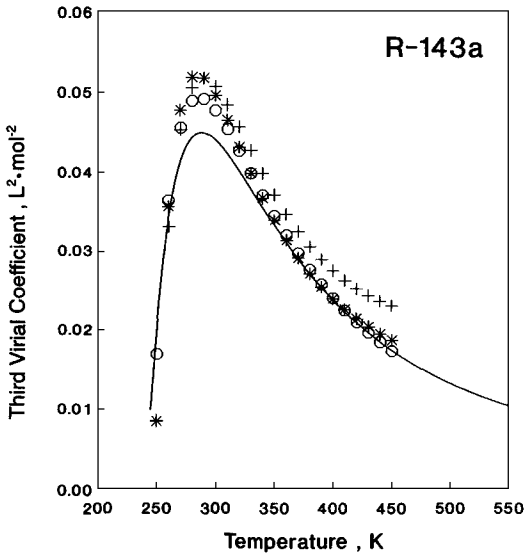

Fig. 18. The third virial coefficients of R-143a. (——) This study; (○) Weber [55]; (*) Zhang [56]; (+) Gillis [15].

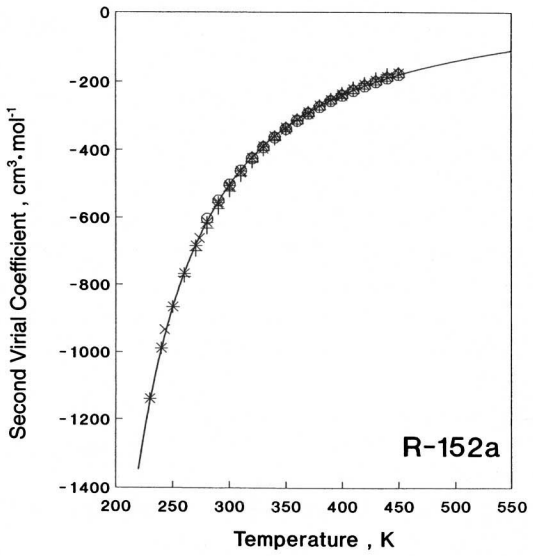

Fig. 19. The second virial coefficients of R-152a. (——) This study; (*) Weber [55]; (○) Tillner-Roth and Baehr [59]; (+) Beckermann and Kohler [25]; (×) Gillis [15]; (△) Zhang [56].

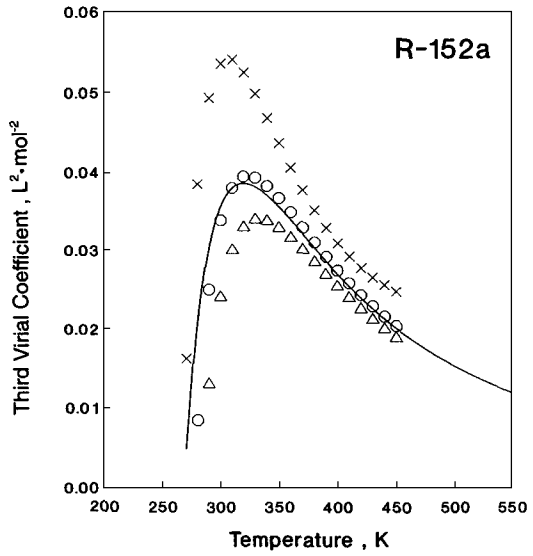

Fig. 20. The third virial coefficients of R-152a. (——) This study; (○) Tillner-Roth and Baehr [59]; (×) Gillis [15]; (△) Weber [55].

R-152a, R-143a, R-134a, R-125, R-32, and R-23 are, 3.93, 3.93, 4.55, 4.55, 3.29, and 3.29 in 10^{-10} m units, respectively, and they compare well with those in Table VIII, within 20% differences. These effective diameters are physically quite acceptable. For the molecular electric dipole moments [48, 49], they are 2.26 (R-152a), 2.35 (R-143a), 2.06 (R-134a), 1.56 (R-125), 1.98 (R-32), and 1.65 (R-23) Debye. The effective dipole moments in Table VIII are also reasonable and only several percent larger than the actual moments, except for R-125, the value of which is 40% larger. Somewhat larger values may indicate that the point-dipole in the model effectively includes higher-order attractive forces such as dipole–quadruple interactions. Finally, concerning the potential well depth, ε/k, it is well-known that for a large number of nonpolar gases, it is related to the critical temperature: roughly $\varepsilon/k = 0.77T_c$. In the present case, they range from $0.63T_c$ to $0.74T_c$ for these polar gases and, thus, seem reasonable.

Therefore, the present potential parameters in Table VIII are physically meaningful quantities. In addition, the calculated reduced Boyle temperatures based on these parameters are from 2.99 to 3.20 for the present molecules, and the maximum inversion temperatures for the zero-pressure Joule–Thomson coefficient range from 5.27 to 5.81 at reduced temperatures. For simple fluids, the Boyle temperature and the inversion temperature correspond to reduced temperatures of about 2.7 and 5.1, respectively. The present values are somewhat larger than those in simple nonpolar gases, and it seems that they are at least semiquantitatively correct. Using the three-term virial equation of state $[Z = 1 + B(T)/V + C(T)/V^2]$, we can make a rough estimate of the vapor–liquid critical temperature. This equation of state has a critical compressibility factor of 1/3, and at the critical point, the relation, $B(T_c)^2 = 3C(T_c)$, holds; T_c can be obtained numerically from this equation. The values agree with the actual critical temperatures within 10%.

ACKNOWLEDGMENTS

The authors are indebted to the New Energy and Industrial Technology Development Organization, Tokyo, for financial support of the present study. They also thank Dr. R. Tillner-Roth for various constructive comments and discussions and Mr. J. Li for his elaborate contribution in preparing the original drawings.

REFERENCES

1. A. S. Rodgers, R. C. Wilhoit, and B. J. Zwolinski, *J. Phys. Chem. Ref. Data* **3**:117 (1974).
2. M. W. Chase, Jr., C. A. Davies, J. R. Downey, Jr., D. J. Frurip, R. A. McDonald, and A. N. Syverud, *J. Phys. Chem. Ref. Data* **14**:Suppl. No. 1 (1985).

3. R. E. Pennington and K. A. Kobe, *J. Chem.* Phys. **22**:1442 (1954).
4. S. S. Chen, A. S. Rodgers, J. Chao, R. C. Wilhoit, and B. J. Zwolinski, *J. Phys. Chem. Ref. Data* **4**:441 (1975).
5. K. S. Pitzer and W. D. Gwinn, *J. Chem.* Phys. **10**:428 (1948).
6. D. A. Long, R. B. Graenor, and D. T. Jones, *Trans. Faraday Soc.* **60**:1509 (1964).
7. R. W. Kirk and P. M. Wilt, *J. Mol. Spectrosc.* **58**:102 (1975).
8. R. Tillner-Roth and A. Yokozeki, *J. Phys. Chem. Ref. Data* **26**:1273 (1997).
9. T. Hozumi, H. Sato, and K. Watanabe, *J. Chem. Eng. Data* **39**:493 (1994).
10. J. R. Nielsen, H. H. Claassen, and N. B. Moran, *J. Chem. Phys.* **23**:329 (1955).
11. S. Kinumaki and M. Kozuka, Bull. *Chem. Soc. Japan* **41**:809 (1968).
12. F. B. Brown, A. D. H.Claugue, N. D. Heitkamp, D. F. Koster, and A. Danti, *J. Mol. Spectrosc.* **24**:163 (1967).
13. D. A. C. Compton and D. M. Rayner, *J. Phys. Chem.* **86**:1628 (1982).
14. J. Chao and A. S. Rodgers, *TRC Thermodynamic Tables Non-Hydorocarbons, VIII* (1989), v-6881.
15. K. A. Gillis, *Int. J. Thermophys.* **18**:73 (1997).
16. T. Hozumi, H. Sato, and K. Watanabe, *Int. J. Thermophys.* **17**:587 (1996).
17. W. F. Edgell, T. R. Riethof, and C. J. Ward, *J. Mol. Spectrosc.* **11**:92 (1963).
18. J. R. Nielsen and C. J. Halley, *J. Mol. Spectrosc.* **17**:341 (1965).
19. A. Danti and J. L. Wood, *J. Chem. Phys.* 30:582 (1959).
20. A. R. H. Goodwin and M. R. Moldover, *J. Chem. Phys.* **93**:2741 (1990).
21. T. Hozumi, H. Sato, and K. Watanabe, *J. Chem. Eng. Data* **41**:1187 (1996).
22. R. S. Basu and D. P. Wilson, *Int. J. Thermophys.* **10**:591 (1989).
23. D. F. Harnish and R. P. Hirschmann, *Appl. Spectrosc.* **24**:28 (1970).
24. P. N. Brier, *J. Mol. Structure* **6**:23 (1970).
25. W. Beckermann and F. Kohler, *Int. J. Thermophys.* **16**:455 (1995).
26. M. Tuerk, M. Crone, and K. Bier, *J. Chem. Thermodyn.* **28**:1179 (1996).
27. M. S. Zhu, L. Z. Han, K. Z. Zhang, and T. Y. Zhou, *Int. J. Thermophys.* **14**:1039 (1990).
28. J. R. Nielsen, H. H. Claassen, and D. C. Smith, *J. Chem. Phys.* **18**:1471 (1950).
29. J. R. Durig, S. M. Craven, K. K. Lau, and J. Bragin, *J. Chem. Phys.* **54**:479 (1971).
30. W. L. Meerts and I. Ozier, *Chem. Phys.* **152**:241 (1991).
31. J. Chao and A. S. Rodgers, *TRC Thermodynamic Tables Non-Hydorocarbons, VIII* (1989), v-6880.
32. R. D. Cowan, G. Herzberg, and S. P. Sinha, *J. Chem. Phys.* **18**:1538 (1950).
33. J. Hatcher and D. M. Yost, *J. Chem. Phys.* **5**:992 (1937).
34. G. T. Fraser, A. S. Pine, J. L. Domench, and B. H. Pate, *J. Chem. Phys.* **99**:2396 (1993).
35. R. Kubo (ed.), *Thermodynamics and Statistical Mechanics* (in Japanese), (Shokabo, Tokyo, 1961), p. 209.
36. D. C. Smith, R. A. Saunders, J. R. Nielsen, and E. E. Ferguson, *J. Chem. Phys.* **20**:847 (1952).
37. W. G. Fately and F. A. Miller, *Spectrochim. Acta* **17**:857 (1961).
38. A. S. Rodgers, *TRC Thermodynamic Tables Non-Hydorocarbons, VIII* (1981), v-6690.
39. T. Hozumi, T. Koga, H. Sato, and K. Watanabe, *Int. J. Thermophys.* **14**:739 (1993).
40. R. M. Villamanan, W. D. Chen, G. Wlodarczak, J. Demaison, A. G. Lesarri, J. C. Lopez, and J. L. Alonso, *J. Mol. Spectrosc.* **171**:223 (1995).
41. J. O. Hirschfelder, C. F. Curtis, and R. B. Bird, *Molecular Theory of Gases and Liquids* (Wiley, New York, 1954).
42. T. Kihara, *Nippon-Sugaku-Busturigakaishi* **17**:11 (1943) (in Japanese).
43. W. H. Stockmayer, *J. Chem. Phys.* **9**:398, 863 (1941).
44. J. S. Rowlinson, *J. Chem. Phys.* **19**:827 (1951).

45. T. Kihara, *J. Phys. Soc. Japan* **3**:265 (1948).
46. R. B. Bird, E. L. Spotz, and J. O. Hirschfelder, *J. Chem. Phys.* **18**:1395 (1950).
47. T. Kihara, *J. Phys. Soc. Japan* **6**:184 (1951).
48. C. W. Meyer and G. Morrison, *J. Phys. Chem.* **95**:3860 (1991).
49. R. C. Reid, J. M. Prausnitz, and B. E. Poling, *The Properties of Gases and Liquids*, 4th ed. (McGraw–Hill, New York, 1987).
50. H. Sutter and R. H. Cole, *J. Chem. Phys.* **52**:132 (1970).
51. H. B. Lange, Jr., and F. P. Stein, *J. Chem. Eng. Data* **15**:56 (1970).
52. B. de Vries, Ph.D. dissertation (University of Hannover, Hannover, 1997).
53. T. Hozumi, Ph.D. dissertation (Keio University, Yokohama, 1997).
54. D. R. Defibaugh, G. Morrison, and L. A. Weber, *J. Chem. Eng. Data* **39**:333 (1994).
55. L. A. Weber, *Int. J. Thermophys.* **15**:461 (1994).
56. H.-L. Zhang, Ph.D. dissertation (Keio University, Yokohama, 1997).
57. S. J. Boyes and L. A. Weber, *J. Chem. Thermodyn.* **27**:163 (1994).
58. C. M. Bignell and P. J. Dunlop, *J. Chem. Phys.* **98**:4889 (1993).
59. R. Tillner-Roth and H.D. Baehr, *J. Chem. Thermodyn.* **24**:413 (1992).